R. & M. No. 3397

MINISTRY OF AVIATION

AERONAUTICAL RESEARCH COUNCIL
REPORTS AND MEMORANDA

Measurements of the Direct Pitching Oscillation Derivatives for Three Cropped Delta and Three Arrowhead Planforms at Subsonic and Transonic Speeds

By C. J. W. MILES and K. B. BRIDGMAN

LONDON: HER MAJESTY'S STATIONERY OFFICE
1965
PRICE 12s. 0d. NET

Measurements of the Direct Pitching Oscillation Derivatives for Three Cropped Delta and Three Arrowhead Planforms at Subsonic and Transonic Speeds

By C. J. W. Miles and K. B. Bridgman

*Reports and Memoranda No. 3397**
August, 1962

Summary.

Measurements of the direct pitching oscillation derivative coefficients on three cropped delta and three arrowhead planforms have been made at subsonic and transonic speeds in the N.P.L. $9\frac{1}{2}$ in. High-Speed Tunnel. The cropped delta wings had aspect ratios of $3 \cdot 0$, $2 \cdot 0$ and $1 \cdot 5$, whilst the arrowheads, of constant aspect ratio $2 \cdot 575$, possessed varying degrees of leading- and trailing-edge sweepback.

The measurements were made about two model axes for each planform and the effects of changing amplitude of oscillation from 2° to 1° have been investigated in the transonic region.

Comparison with subsonic theory is reasonably good for the damping and stiffness derivative coefficients measured about the forward axis but agreement for the latter coefficients is poorer for all the rearward axis positions.

1. *Introduction.*

The measurements described in this report are part of a general programme of derivative tests being made in the N.P.L. $9\frac{1}{2}$ in. High-Speed Tunnel. Some similar experiments with a cropped delta wing of aspect ratio $1 \cdot 8$ using the same apparatus have already been completed and were discussed in an earlier report[1].

In general a Mach number range from $0 \cdot 4$ to $1 \cdot 12$ was covered, tests being made at zero mean incidence and at an amplitude of oscillation of 2°. Some tests were made at 1° amplitude over a smaller range of Mach number close to $M = 1 \cdot 0$. The direct derivatives m_α and $m_{\dot{\alpha}}$ were measured at a frequency of about 25 c/s, but tests on the cropped delta wing of aspect ratio $3 \cdot 0$ were repeated at 50 c/s approximately in order to examine the effect of higher frequency parameter. Originally it had been decided to repeat the tests at 50 c/s for all six wings, but the relatively large size of the apparatus damping at this frequency would have made some of the measurements of $m_{\dot{\alpha}}$ inaccurate. In any case results for the aspect ratio $3 \cdot 0$ cropped delta showed only small differences from those at the lower frequency.

Some attention was paid to the problem of slotted-wall interference effects by closing some of the existing slots and also by repeating part of the investigation with a second pair of walls having wider slots and slats.

* Replaces N.P.L. Aero Report No. 1033—A.R.C. 23 990. Published with the permission of the Director, National Physical Laboratory.

2. *Technique of Measurement.*

The apparatus used employed an electrically self-excited system shown in Fig. 19 and described in detail in Ref. 2, but for the present tests the apparatus inner frame was clamped to the earthed structure.

The stiffness derivative coefficient m_α was measured by observing the change of frequency of the oscillating system on running the tunnel, whilst the damping derivative coefficient $m_{\dot{\alpha}}$ was obtained by measuring the difference in the electrical power input to the exciter coils to maintain constant amplitude with and without the wind.

A different method was used, however, for the calculation of the stiffness derivative from the observations. In the earlier experiment three constants A, B and C, in a formula for calculating m_α, were determined by simulating three different values of the latter by adding inertias at the model end, and subsequently solving a set of simultaneous equations. This method led to inaccuracies in the values for m_α, in some instances, due to the equations being ill-conditioned.

For the present tests these constants were evaluated by using a knowledge of the position of the node in the torsion bar, obtained by measuring the amplitudes of oscillation at the two ends, and the elastic stiffnesses associated with the system.

3. *Corrections to Measurements.*

No tunnel corrections have been applied to any of the results given in this paper. Other corrections arise from the oscillating apparatus itself and have been discussed in detail in Ref. 3.

3.1. *Leakage of Air into Apparatus Box.*

Original difficulties in sealing the apparatus box[3] were overcome before commencing this series of tests, and the very small leak remaining was considered to have no measurable effect on the results.

3.2. *Air Density in Apparatus Box.*

These corrections arise since the power datum is obtained with atmospheric pressure in the apparatus box, whilst for strict accuracy the pressure should be that which obtains during the wind-on measurement and with zero still-air damping on the model. The frequency datum should relate to the wind-on pressure condition, but should include the still-air virtual inertia on the model and moving parts in the apparatus box. The magnitude of the errors involved was investigated by placing a cover box over the model and measuring the power and frequency with the box evacuated to various pressures.

The result of these tests was that errors in the datum conditions due to the air density of the apparatus box were negligible.

3.3. *Effect of Mode on Apparatus Damping.*

A further error is involved in taking the still-air power as a datum for the damping derivative measurement, since when the tunnel is running a different mode of vibration exists in which the position of the node in the torsion bar (Fig. 19) moves, due to the aerodynamic loading on the model. The following method was used to determine the magnitude of this correction, the assumption being that apparatus damping was due to hysteresis losses.

Still-air tests were made in which various inertias were added to the oscillating apparatus at the model end, and corresponding measurements of damping and frequency were made. A graph of damping against frequency gave a smooth curve which was then used to modify the value of the apparatus damping measured in still air to that required for the wind-on condition, since the wind-on frequency was known.

The corrections produced by this method for the damping derivative $m_{\dot{\alpha}}$ varied rather widely but did not exceed about 10% of the uncorrected value.

4. *Details of Models.*

The six half-span aerofoils consisted of two separate families, all with an RAE 102 section and a maximum $t/c = 0 \cdot 06$. The aspect ratio of the cropped-delta family ranged between $3 \cdot 0$ and $1 \cdot 5$ with a constant taper ratio, whilst the arrowhead series had leading-edge sweepback angles of between $33 \cdot 7°$ and $59 \cdot 0°$ with both aspect ratio and taper ratio remaining constant. A small manufacturing error in arrowhead No. 3 explains the presence of insignificant dimensional differences from the other two members of the family.

The models were made of solid steel each being fitted at the root with a fence in the form of a thin metal plate 0·020 in. thick. The purposes of this fence were to reduce the effects of flow through the narrow gap between the aerofoil root and the tunnel wall and through the hole in the wall which accommodates a tongue, extending from the root of the model to the oscillating apparatus. Previous measurements of the effects of various sizes of fence, had shown that the size was not critical below $M = 1 \cdot 0$ provided that this hole was covered. For each aerofoil tested a fence was designed sufficiently large to comply with this condition.

The six planforms are sketched in Figs. 1 and 2 where the axis positions are also shown. Complete data for all the models are given in Table 1.

5. *Experimental Results.*

5.1. *Measurements of m_α, $m_{\dot{\alpha}}$.*

Values of $-m_\alpha$ and $-m_{\dot{\alpha}}$ plotted against Mach number are shown in Figs. 3 to 9 (inclusive) for the cropped delta wings and Figs. 10 to 15 (inclusive) for the arrowheads.

For the cropped delta wings in the forward axis position the stiffness derivative coefficient $-m_\alpha$ shows little change in value up to Mach numbers of about 0·9. For values of M above 0·9 $-m_\alpha$ increases quite rapidly but the increase is delayed progressively with increasing leading-edge sweep (Figs. 3a, 4a and 5a). For the rearward axis (Figs. 3b, 4b and 5b) there is a small numerical increase in the value of $-m_\alpha$ up to $M = 0 \cdot 9$ approximately. At higher Mach numbers there is a marked change in direction and once again the onset of the change is delayed with increasing sweep of the leading edge.

The damping derivative coefficient $-m_{\dot{\alpha}}$ for the forward axis shows little variation up to about $M = 0 \cdot 8$ (Figs. 6a, 7a and 8a), but at higher Mach numbers the derivative rises rapidly to a peak and then falls. With increasing sweepback this peak occurs at a higher speed and becomes less pronounced. The value of $-m_{\dot{\alpha}}$ measured about the rearward axis (Figs. 6b, 7b and 8b) shows a rise with increasing Mach number from $M = 0 \cdot 4$. Between $M = 0 \cdot 8$ and $M = 0 \cdot 9$ the derivative ceases to increase temporarily but at still higher speeds a peak value is attained. This peak again occurs at a higher Mach number and decreases numerically with increased leading-edge sweep. For each of the three cropped delta wings the peak value of $-m_{\dot{\alpha}}$ occurs at the same Mach number for both axis positions.

In the case of the arrowhead family measured about the forward axis position the curve of stiffness derivative coefficient $-m_\alpha$ against Mach number (Figs. 10a, 11a and 12a) is similar to the cropped-delta curve in showing little change at low Mach numbers and then rising sharply at higher speeds. The peak is delayed with increasing L.E. sweepback and for arrowhead No. 3 is not reached at $M = 1 \cdot 12$, the highest Mach number obtainable. For the rearward axis $-m_\alpha$ shows a modest numerical increase at low Mach numbers followed by a more rapid decrease at higher speeds (Figs. 10b, 11b and 12b).

The damping derivative coefficient $-m_{\dot\alpha}$ measured about the forward axis (Figs. 13a, 14a and 15a) shows a tendency to fall at Mach numbers up to about $0 \cdot 8$. Above $M = 0 \cdot 8$ there is a peak which is delayed by increased sweepback and for the arrowhead with most sweep the maximum is not reached. Values of $-m_{\dot\alpha}$ measured about the rearward axis (Figs. 13b, 14b and 15b) increase fairly steadily with Mach number up to about $M = 0 \cdot 95$ when there is a small decrease. With the exception of the model with most sweepback there follows a large increase in the value of $-m_{\dot\alpha}$ at the highest speed attainable ($M = 1 \cdot 12$).

5.2. *Effects of Amplitude.*

The majority of the measurements of m_α and $m_{\dot\alpha}$ were made using an amplitude of oscillation of about 2°, but many tests were repeated at 1° amplitude over a Mach number range of $0 \cdot 9$ to $1 \cdot 1$ {Figs. 3 to 15 (inclusive)}. The effects of amplitude appear in all cases to be small.

5.3. *Effects of Frequency.*

The tests were in general made at about 25 c/s since at the higher frequencies available the apparatus damping tended to become large compared with the aerodynamic damping. Some measurements of m_α and $m_{\dot\alpha}$ were made, however, at 51 c/s on the cropped delta of A.R. $3 \cdot 0$ for the forward axis (Figs. 9a, 9b). Comparison of these curves with Figs. 3a and 6a respectively shows that the effects of frequency are small.

5.4. *Effects of Transition.*

Almost all the experiments were carried out with free transition and laminar boundary layer, but a few measurements of m_α and $m_{\dot\alpha}$ were made with turbulent boundary layer on arrowhead No. 2 wing for the rearward axis, transition being fixed by means of strips of carborundum powder on both upper and lower surfaces at the wing leading edge. The effect of making the boundary layer turbulent is shown in Figs. 16a, 16b and can be seen to be small.

5.5. *Effects of Tunnel Wall Interference.*

In order to obtain some experimental data for the effects of slotted-wall tunnel interference on the measurements of m_α and $m_{\dot\alpha}$ tests were repeated for the cropped delta wing of aspect ratio $3 \cdot 0$, using the forward axis at a frequency of 51 c/s and 2° amplitude. In this repeat experiment four wall conditions were examined, as follows:

(i) The original slotted walls consisting of 16 slats each $\frac{1}{2}$ in. wide alternating with 15 slots each 3/32 in. wide with 2 end slots of 3/64 in. width.

(ii) Eight alternate slots were then covered by means of tape, making the open/closed ratio equal to half its original value.

(iii) The walls were completely sealed by covering the remaining slots with tape, thus making a closed-wall tunnel.

(iv) Another pair of walls was used, each having 4 slats $1\frac{1}{2}$ in. wide together with one at each end 1 in. wide, and 5 slots each 9/32 in. across. The open/closed ratio remained substantially the same as in (i).

The results for m_{α} and $m_{\dot{\alpha}}$ obtained with these conditions are shown in Figs. 17a and 17b. Progressive sealing of the slots gives increasing values of $-m_{\alpha}$ and decreasing values of $-m_{\dot{\alpha}}$, but the effect on the damping is much smaller at the higher Mach numbers. Results of the derivatives obtained for the walls with wider slots and slats (iv), agree generally with those obtained using narrower slots (i) and (ii). Values of $-m_{\alpha}$ for the closed-wall condition (iii) were corrected for tunnel wall interference using conventional solid-wall theory and gave reasonably good agreement with the slotted-wall cases (i) and (ii). Some tests were repeated at 27 c/s for the normal slotted walls and for the completely sealed walls, conditions (i) and (iii) above (Figs. 18a and 18b). In both cases the values of $-m_{\alpha}$ and $-m_{\dot{\alpha}}$ are in good agreement with the corresponding values obtained at 51 c/s (Figs. 17a and 17b).

Static tests on tunnel wall interference in another N.P.L. high-speed tunnel[5] have shown that the interference depends on a theoretical parameter T, where

$$T = \frac{1 - \dfrac{C}{H}}{1 + \dfrac{C}{H}},$$

H = tunnel height between slotted walls,

$$C = -\frac{2l}{\pi} \log_e \sin \frac{\pi\sigma}{2},$$

$2l$ = the slot spacing,

σ = open area/closed area.

The values of T for the normal walls with 8 slots sealed (ii) and for the walls with wider slots (iv) were nearly equal. It will be noted that the values of $-m_{\alpha}$ and $-m_{\dot{\alpha}}$ for these two conditions are practically identical, except above $M = 1 \cdot 0$.

Shortage of time prevented further slotted-wall interference tests but it would seem that the original wall condition was not critical for the results of m_{α} and $m_{\dot{\alpha}}$ presented here.

6. *Comparisons with Theory.*

Subsonic theoretical values of the derivative coefficients relating to a pitching oscillation have been obtained for all six planforms by Acum and Garner[6] and are shown in Figs. 3 to 15 (inclusive).

The stiffness derivative $-m_{\alpha}$ measured for the forward axis shows quite good agreement at the lower Mach numbers. At higher speeds the experimental values are consistently smaller numerically, the difference being less in the case of the arrowheads. In the rearward axis position the experimental results of $-m_{\alpha}$ are always smaller than theory, although in every case the trends with Mach number are the same.

The damping derivative $-m_{\dot{\alpha}}$ measured for the forward axis shows similarities to the stiffness derivative in that the agreement with theory is reasonable at low Mach numbers. Again experiment falls below theory at higher speeds, although the results for the arrowheads agree rather better than those for the deltas. For the rearward axis the measured values of $-m_{\dot{\alpha}}$ are consistently larger at Mach numbers near $0 \cdot 7$ to $0 \cdot 8$ but at higher speeds experiment falls markedly below the theoretical value.

7. *Conclusions.*

(1) For all six aerofoils the stiffness derivative coefficient m_{α} varies only slightly over the Mach number range of $0 \cdot 4$ to $0 \cdot 8$. At higher speeds more marked changes occur, with forward axis measurements showing larger changes than those for the rearward axis. The damping derivative coefficient $m_{\dot{\alpha}}$ shows larger variations with Mach number, in some cases starting from $M = 0 \cdot 4$. Where peaks are observed their positions with respect to Mach number vary progressively with leading-edge sweep.

(2) The effects of amplitude, frequency and turbulent boundary layer for the cases investigated are small.

(3) Some tests have been made in an attempt to determine the effects on the measurements of slotted-wall tunnel interference but more data are required to reach a valid conclusion.

(4) Comparisons with subsonic theory are generally reasonable, with poorer agreement in some cases at the higher Mach numbers. The relation between theory and experiment is remarkably consistent.

8. *Further Tests.*

Experimental work planned for the future in the $9\frac{1}{2}$ in. Tunnel involves the measurement of pitching oscillation derivatives for complete slender delta planforms at transonic speeds using a sting-mounted rig.

Acknowledgement.

The authors wish to acknowledge the assistance given by Mr. J. B. Bratt, both in the experimental work and the preparation of this report.

NOTATION

The complex pitching moment relating to a pitching oscillation is given by:

$$\mathscr{M} = \rho V^2 S\bar{c}(m_\alpha + j\omega m_{\dot{\alpha}})\alpha$$

where the symbols are defined below,

$\mathscr{M}$	Pitching moment (positive nose up)
c_0	Root chord
$\bar{c}$	Mean chord
f	Frequency of oscillation
h	Distance of axis downstream of apex, as fraction of c_0
M	Mach number
S	Area of wing
V	Wind speed
α	Pitching displacement (positive nose up)
α_0	Amplitude of oscillation
ρ	Air density (free stream)
ω	Frequency parameter $(=2\pi f\bar{c}/V)$
$\left.\begin{matrix} m_\alpha \\ m_{\dot{\alpha}} \end{matrix}\right\}$	Non-dimensional derivative coefficients as defined in Ref. 4.

REFERENCES

No.	Author(s)	Title, etc.
1	C. J. W. Miles, J. B. Bratt and K. B. Bridgman.	Measurements of pitching oscillation derivatives at subsonic and transonic speeds for a cropped delta wing of aspect ratio 1·8 (Interim Report). A.R.C. C.P. 534. February, 1960.
2	J. B. Bratt	A note on derivative apparatus for the N.P.L. $9\frac{1}{2}$ inch High-Speed Tunnel. A.R.C. C.P. 269. January, 1956.
3	J. B. Bratt, C. J. W. Miles and R. F. Johnson.	Measurements of the direct hinge-moment derivatives at subsonic and transonic speeds for a cropped delta wing with oscillating flap. A.R.C. R. & M. 3163. May, 1957.
4	I. T. Minhinnick	Tables of functions for evaluation of wing and control surface flutter derivatives for incompressible flow. A.R.C. 13 730. July, 1950.
5	H. H. Pearcey, C. S. Sinnott and J. Osborne.	Some effects of wind-tunnel interference observed in tests on two-dimensional aerofoils at high subsonic and transonic speeds. N.P.L. Aero. Note 373. 1959.
6	W. E. A. Acum and H. C. Garner	The estimation of oscillatory wing and control derivatives. A.R.C. C.P. 623. March, 1961.

TABLE 1

Details of Models

The data relate to complete models.

(a) *Cropped-Delta Family.*

Aspect ratio	3·0	2·0	1·5
Taper ratio	0·143	0·143	0·143
Thickness/chord ratio	0·06	0·06	0·06
Section	RAE 102	RAE 102	RAE 102
Apex angle	90·0°	67·37°	53·13°
Sweepback (L.E.)	45·0°	56·31°	63·43°
Sweepback (T.E.)	0°	0°	0°
Span	6·858 in.	7·000 in.	6·000 in.
Root chord	4·000 in.	6·125 in.	7·000 in.
Tip chord	0·571 in.	0·875 in.	1·000 in.
Mean chord	2·285 in.	3·500 in.	4·000 in.
Axis position h (forward)	0·2435	0·3519	0·3774
Axis position h (rearward)	0·8685	0·7601	0·7346

TABLE 1—*continued*

(b) *Arrowhead Family.*

Arrowhead	No. 1	No. 2	No. 3*
Aspect ratio	2·64	2·64	2·67
Taper ratio	0·389	0·389	0·389
Thickness/chord ratio	0·06	0·06	0·06
Section	RAE 102	RAE 102	RAE 102
Apex angle	112·63°	81·20°	61·94°
Sweepback (L.E.)	33·68°	49·40°	59·03°
Sweepback (T.E.)	0°	26·58°	45·20°
Span	7·334 in.	7·334 in.	7·334 in.
Root chord	4·000 in.	4·000 in.	3·958 in.
Tip chord	1·555 in.	1·555 in.	1·539 in.
Mean chord	2·778 in.	2·778 in.	2·748 in.
Axis position h (forward)	0·1535	0·3535	0·5493
Axis position h (rearward)	0·7785	0·9785	1·1809

* The dimensions of this model were slightly non-standard due to an error in manufacture.

TABLE 2

Aspect Ratio 3·0 *Delta*

$h = 0{\cdot}2435$, $f = 27$ c/s (nominal)

M	α_0 (deg)	ω	$-m_{\dot{\alpha}}$	$-m_\alpha$	α_0 (deg)	ω	$-m_{\dot{\alpha}}$	$-m_\alpha$
0·397	2·08	0·0744	1·474	0·836	1·05	0·0747	1·466	0·838
0·397	2·08	0·0746	1·470	0·813				
0·597	2·09	0·0510	1·519	0·807	1·05	0·0509	1·563	0·816
0·695	2·23	0·0445	1·477	0·835				
0·695	2·10	0·0443	1·507	0·839				
0·795	2·08	0·0393	1·604	0·869				
0·844	2·09	0·0377	1·610	0·881	1·04	0·0378	1·599	0·868
0·844	2·10	0·0379	1·657	0·876				
0·870	2·06	0·0366	1·745	0·886				
0·896	2·08	0·0356	1·874	0·899				
0·920	2·07	0·0351	2·183	0·931	1·03	0·0350	2·224	0·928
0·920	2·13	0·0351	2·085	0·933	1·05	0·0350	2·181	0·934
0·946	2·08	0·0344	1·957	1·040				
0·946	2·09	0·0343	2·035	1·030				
0·969	2·06	0·0336	1·580	1·177				
0·969	2·10	0·0339	1·482	1·164				
0·994	2·06	0·0331	1·367	1·235	1·03	0·0331	1·164	1·208
0·994	2·08	0·0330	1·156	1·257				
1·042	2·07	0·0318	1·012	1·233				
1·042	2·11	0·0318	1·060	1·244	1·05	0·0319	1·079	1·185
1·092	2·06	0·0308	0·973	1·166	1·05	0·0307	{ 1·077	1·079
1·092	2·12	0·0308	0·874	1·166			1·122	
1·092					1·06	0·0307	1·124	1·079
1·117	2·08	0·0300	1·068	1·123	1·04	0·0301	1·055	1·027
1·117	2·12	0·0301	1·281	1·128				

$h = 0{\cdot}8685$, $f = 25$ c/s (nominal)

M	α_0 (deg)	ω	$-m_{\dot{\alpha}}$	$-m_\alpha$
0·397	2·08	0·0691	0·204	−0·788
0·597	2·09	0·0466	0·394	−0·806
0·597	2·13	0·0463	0·333	−0·797
0·695	2·13	0·0403	0·731	−0·825
0·795	2·04	0·0357	1·114	−0·854
0·795	2·09	0·0358	1·021	−0·843
0·844	2·14	0·0337	1·059	−0·866
0·896	2·10	0·0320	1·099	−0·879
0·896	2·14	0·0319	1·049	−0·872
0·920	2·04	0·0314	1·252	−0·879
0·946	1·92	0·0306	1·256	−0·860
0·946	2·05	0·0306	1·172	−0·858
0·969	2·04	0·0301	1·130	−0·821
0·994	2·05	0·0294	0·997	−0·785
0·994	2·14	0·0292	0·954	−0·780
1·042	1·95	0·0282	0·928	−0·768
1·092	1·96	0·0272	1·168	−0·748
1·092	2·13	0·0271	1·108	−0·737
1·117	2·05	0·0267	1·255	−0·739

TABLE 2—*continued*

Aspect Ratio 2·0 Delta

$h = 0·3519$, $f = 27$ c/s (nominal)

M	α_0 (deg)	ω	$-m_{\dot{\alpha}}$	$-m_{\alpha}$	α_0 (deg)	ω	$-m_{\dot{\alpha}}$	$-m_{\alpha}$
0·397	2·01	0·1117	0·891	0·400				
0·397	2·04	0·1107	0·878	0·402				
0·597	2·00	0·0770	0·865	0·390				
0·795	2·02	0·0592	0·810	0·404				
0·844	2·04	0·0554	0·826	0·403				
0·896	2·02	0·0534	0·847	0·412	1·00	0·0534	0·914	0·409
0·920	2·05	0·0516	0·946	0·404				
0·946	2·02	0·0506	1·135	0·424	1·00	0·0511	1·195	0·423
0·969	1·99	0·0502	1·201	0·426				
0·969	2·03	0·0495	1·225	0·429				
0·994	2·02	0·0493	1·202	0·489	1·00	0·0492	1·244	0·484
1·018	2·00	0·0487	1·145 1·069	0·545	1·00	0·0483	1·092	0·558
1·042	1·98	0·0478	1·158	0·598	1·00	0·0479	1·277	0·599
1·067	1·82	0·0470	1·248	0·599				
1·067	2·00	0·0469	1·279	0·603				
1·092	1·82	0·0461	1·162	0·593	0·99	0·0462	1·174	0·576
1·092					1·00	0·0457	1·203	0·580
1·117	1·83	0·0453	1·061	0·601	0·98	0·0452	1·036	0·575
1·117	1·97	0·0453	1·087	0·603				

$h = 0·7601$, $f = 26$ c/s (nominal)

M	α_0 (deg)	ω	$-m_{\dot{\alpha}}$	$-m_{\alpha}$	α_0 (deg)	ω	$-m_{\dot{\alpha}}$	$-m_{\alpha}$
0·397	1·96	0·1100	0·074	−0·377				
0·597	1·98	0·0744	0·163	−0·385				
0·646	2·05	0·0686	0·222	−0·391				
0·695	2·03	0·0641	0·297	−0·392				
0·746	1·97	0·0600	0·366	−0·392				
0·770	2·04	0·0582	0·366	−0·395				
0·795	1·96	0·0567	0·379	−0·399				
0·844	1·98	0·0539	0·408	−0·403				
0·870	1·99	0·0521	0·418	−0·411				
0·896	1·97	0·0511	0·384	−0·411	1·02	0·0512	0·416	−0·416
0·896	1·99	0·0506	0·415	−0·411				
0·920	1·99	0·0496	0·409	−0·416				
0·946	1·98	0·0489	0·475	−0·417	1·00	0·0482	0·462	−0·417
0·969	1·98	0·0477	0·541	−0·413				
0·994	1·97	0·0468	0·555	−0·391	1·00	0·0466	0·587	−0·398
0·994	1·99	0·0462	0·522	−0·391				
1·108	1·97	0·0458	0·455	−0·360				
1·042	1·97	0·0452	0·375	−0·332	0·98	0·0450	0·361	−0·324
1·092	1·99	0·0432	0·331	−0·312	1·01	0·0434	0·326	−0·306
1·092	1·99	0·0432	0·326	−0·310				
1·117	2·00	0·0428	0·345	−0·312				

TABLE 2

Aspect Ratio 3·0 *Delta*

$h = 0{\cdot}2435$, $f = 27$ c/s (nominal)

M	α_0 (deg)	ω	$-m_{\dot{\alpha}}$	$-m_\alpha$	α_0 (deg)	ω	$-m_{\dot{\alpha}}$	$-m_\alpha$
0·397	2·08	0·0744	1·474	0·836	1·05	0·0747	1·466	0·838
0·397	2·08	0·0746	1·470	0·813				
0·597	2·09	0·0510	1·519	0·807	1·05	0·0509	1·563	0·816
0·695	2·23	0·0445	1·477	0·835				
0·695	2·10	0·0443	1·507	0·839				
0·795	2·08	0·0393	1·604	0·869				
0·844	2·09	0·0377	1·610	0·881	1·04	0·0378	1·599	0·868
0·844	2·10	0·0379	1·657	0·876				
0·870	2·06	0·0366	1·745	0·886				
0·896	2·08	0·0356	1·874	0·899				
0·920	2·07	0·0351	2·183	0·931	1·03	0·0350	2·224	0·928
0·920	2·13	0·0351	2·085	0·933	1·05	0·0350	2·181	0·934
0·946	2·08	0·0344	1·957	1·040				
0·946	2·09	0·0343	2·035	1·030				
0·969	2·06	0·0336	1·580	1·177				
0·969	2·10	0·0339	1·482	1·164				
0·994	2·06	0·0331	1·367	1·235	1·03	0·0331	1·164	1·208
0·994	2·08	0·0330	1·156	1·257				
1·042	2·07	0·0318	1·012	1·233				
1·042	2·11	0·0318	1·060	1·244	1·05	0·0319	1·079	1·185
1·092	2·06	0·0308	0·973	1·166	1·05	0·0307	1·077	1·079
1·092	2·12	0·0308	0·874	1·166			1·122	
1·092					1·06	0·0307	1·124	1·079
1·117	2·08	0·0300	1·068	1·123	1·04	0·0301	1·055	1·027
1·117	2·12	0·0301	1·281	1·128				

$h = 0{\cdot}8685$, $f = 25$ c/s (nominal)

M	α_0 (deg)	ω	$-m_{\dot{\alpha}}$	$-m_\alpha$
0·397	2·08	0·0691	0·204	−0·788
0·597	2·09	0·0466	0·394	−0·806
0·597	2·13	0·0463	0·333	−0·797
0·695	2·13	0·0403	0·731	−0·825
0·795	2·04	0·0357	1·114	−0·854
0·795	2·09	0·0358	1·021	−0·843
0·844	2·14	0·0337	1·059	−0·866
0·896	2·10	0·0320	1·099	−0·879
0·896	2·14	0·0319	1·049	−0·872
0·920	2·04	0·0314	1·252	−0·879
0·946	1·92	0·0306	1·256	−0·860
0·946	2·05	0·0306	1·172	−0·858
0·969	2·04	0·0301	1·130	−0·821
0·994	2·05	0·0294	0·997	−0·785
0·994	2·14	0·0292	0·954	−0·780
1·042	1·95	0·0282	0·928	−0·768
1·092	1·96	0·0272	1·168	−0·748
1·092	2·13	0·0271	1·108	−0·737
1·117	2·05	0·0267	1·255	−0·739

TABLE 2—*continued*

Aspect Ratio 2·0 Delta

$h = 0·3519$, $f = 27$ c/s (nominal)

M	α_0 (deg)	ω	$-m_{\dot{\alpha}}$	$-m_{\alpha}$	α_0 (deg)	ω	$-m_{\dot{\alpha}}$	$-m_{\alpha}$
0·397	2·01	0·1117	0·891	0·400				
0·397	2·04	0·1107	0·878	0·402				
0·597	2·00	0·0770	0·865	0·390				
0·795	2·02	0·0592	0·810	0·404				
0·844	2·04	0·0554	0·826	0·403				
0·896	2·02	0·0534	0·847	0·412	1·00	0·0534	0·914	0·409
0·920	2·05	0·0516	0·946	0·404				
0·946	2·02	0·0506	1·135	0·424	1·00	0·0511	1·195	0·423
0·969	1·99	0·0502	1·201	0·426				
0·969	2·03	0·0495	1·225	0·429				
0·994	2·02	0·0493	1·202	0·489	1·00	0·0492	1·244	0·484
1·018	2·00	0·0487	1·145 1·069	0·545	1·00	0·0483	1·092	0·558
1·042	1·98	0·0478	1·158	0·598	1·00	0·0479	1·277	0·599
1·067	1·82	0·0470	1·248	0·599				
1·067	2·00	0·0469	1·279	0·603				
1·092	1·82	0·0461	1·162	0·593	0·99	0·0462	1·174	0·576
1·092					1·00	0·0457	1·203	0·580
1·117	1·83	0·0453	1·061	0·601	0·98	0·0452	1·036	0·575
1·117	1·97	0·0453	1·087	0·603				

$h = 0·7601$, $f = 26$ c/s (nominal)

M	α_0 (deg)	ω	$-m_{\dot{\alpha}}$	$-m_{\alpha}$	α_0 (deg)	ω	$-m_{\dot{\alpha}}$	$-m_{\alpha}$
0·397	1·96	0·1100	0·074	−0·377				
0·597	1·98	0·0744	0·163	−0·385				
0·646	2·05	0·0686	0·222	−0·391				
0·695	2·03	0·0641	0·297	−0·392				
0·746	1·97	0·0600	0·366	−0·392				
0·770	2·04	0·0582	0·366	−0·395				
0·795	1·96	0·0567	0·379	−0·399				
0·844	1·98	0·0539	0·408	−0·403				
0·870	1·99	0·0521	0·418	−0·411				
0·896	1·97	0·0511	0·384	−0·411	1·02	0·0512	0·416	−0·416
0·896	1·99	0·0506	0·415	−0·411				
0·920	1·99	0·0496	0·409	−0·416				
0·946	1·98	0·0489	0·475	−0·417	1·00	0·0482	0·462	−0·417
0·969	1·98	0·0477	0·541	−0·413				
0·994	1·97	0·0468	0·555	−0·391	1·00	0·0466	0·587	−0·398
0·994	1·99	0·0462	0·522	−0·391				
1·108	1·97	0·0458	0·455	−0·360				
1·042	1·97	0·0452	0·375	−0·332	0·98	0·0450	0·361	−0·324
1·092	1·99	0·0432	0·331	−0·312	1·01	0·0434	0·326	−0·306
1·092	1·99	0·0432	0·326	−0·310				
1·117	2·00	0·0428	0·345	−0·312				

TABLE 2—*continued*

Aspect Ratio 1·5 *Delta*

$h = 0\cdot3774$, $f = 26$ c/s (nominal)

M	α_0 (deg)	ω	$-m_{\dot{\alpha}}$	$-m_{\alpha}$	α_0 (deg)	ω	$-m_{\dot{\alpha}}$	$-m_{\alpha}$
0·397	2·00	0·1270	0·734	0·307				
0·397	2·01	0·1270	0·739	0·301				
0·597	2·02	0·0868	0·743	0·317				
0·795	2·03	0·0671	0·735	0·322				
0·844	1·97	0·0639	0·758	0·315				
0·896	2·01	0·0617	0·835	0·320	1·01	0·0527	0·891	0·313
0·946	2·04	0·0583	0·925	0·329	1·00	0·0505	0·952	0·324
0·994	2·03	0·0559	0·981	0·360	0·99	0·0485	1·117	0·328
0·994	2·04	0·0561	1·014	0·342				
1·018	1·96	0·0548	0·999	0·365				
1·042	2·00	0·0542	0·895	0·423	0·99	0·0470	0·996	0·419
1·067	1·95	0·0532	0·875	0·443				
1·092	1·88	0·0524	0·936	0·468	1·00	0·0454	0·959	0·460
1·092	2·02	0·0522	0·931	0·471				
1·117	2·03	0·0512	1·028	0·459				

$h = 0\cdot7346$, $f = 25$ c/s (nominal)

M	α_0 (deg)	ω	$-m_{\dot{\alpha}}$	$-m_{\alpha}$	α_0 (deg)	ω	$-m_{\dot{\alpha}}$	$-m_{\alpha}$
0·397	2·00	0·1196	0·093	−0·267				
0·597	1·80	0·0803	0·144	−0·276				
0·597	2·01	0·0817	0·149	−0·280				
0·795	2·02	0·0618	0·262	−0·279				
0·896	2·03	0·0554	0·366	−0·284	1·00	0·0489	0·388	−0·295
0·896	1·83	0·0489	0·338	−0·296				
0·908	1·88	0·0546	0·317	−0·284				
0·920	1·90	0·0541	0·286	−0·284				
			0·300					
0·946	1·88	0·0527	0·338	−0·286	1·00	0·0471	0·372	−0·295
0·946	2·03	0·0528	0·327	−0·284				
0·969	1·90	0·0515	0·395	−0·289				
0·994	2·03	0·0506	0·454	−0·284	1·00	0·0449	0·511	−0·295
1·006	1·88	0·0500	0·443	−0·281				
1·018	1·90	0·0496	0·447	−0·267				
1·042	1·85	0·0491	0·320	−0·237	1·00	0·0433	0·386	−0·242
1·067	1·81	0·0479	0·264	−0·209				
1·067	1·90	0·0478	0·253	−0·208				
1·092	1·84	0·0474	0·239	−0·195	1·00	0·0417	0·206	−0·197
1·117	1·83	0·0467	0·273	−0·193				

TABLE 2—*continued*

Aspect Ratio 3·0 *Delta*

$h = 0{\cdot}2435, f = 51$ c/s (nominal)

M	α_0 (deg)	ω	$-m_{\dot{\alpha}}$	$-m_{\alpha}$	α_0 (deg)	ω	$-m_{\dot{\alpha}}$	$-m_{\alpha}$
0·397	2·04	0·1400	1·654	0·850	1·02	0·1407	1·682	0·870
0·397	2·10	0·1400	1·627	0·850				
0·597	2·05	0·0950	1·753	0·821	1·02	0·0955	1·696	0·842
0·597	2·06	0·0954	1·696	0·845				
0·695	2·07	0·0824	1·672	0·865				
0·695	2·08	0·0826	1·744	0·866				
0·795	2·06	0·0734	1·724	0·895				
0·844	2·08	0·0695	1·825	0·916	1·03	0·0695	1·830	0·886
0·896	2·06	0·0660	1·988	0·928				
0·896	2·07	0·0659	1·999	0·927				
0·920	2·08	0·0648	2·132	0·964	1·03	0·0649	2·151	0·952
0·933	2·03	0·0645	2·130	0·984	1·04	0·0639	2·256	0·984
0·933	2·05	0·0642	2·120	0·986				
0·946	2·05	0·0634	2·133	1·046				
0·946	2·07	0·0631	2·188	1·048				
0·969	2·08	0·0620	1·717	1·190				
0·994	2·04	0·0608	1·245	1·273	1·03	0·0607	1·398	1·237
0·994	2·07	0·0606	1·320	1·269				
1·042	2·04	0·0585	1·003	1·273	1·03	0·0585	1·217	1·193
1·042	2·06	0·0584	1·119	1·268				
1·067	2·08	0·0573	0·986	1·234				
1·092	2·03	0·0567	0·882	1·192	1·03	0·0564	0·909	1·095
1·092	2·07	0·0562	0·839	1·200	1·03	0·0567	1·045	1·112
1·117	2·07	0·0552	0·870	1·151	1·03	0·0554	1·218	1·054
1·117					1·03	0·0558	1·263	1·051

TABLE 2—*continued*

Arrowhead No. 1 *L.E. Sweep* 33·68°

$h = 0\cdot1535, f = 28$ c/s (nominal)

M	α_0 (deg)	ω	$-m_{\dot{\alpha}}$	$-m_{\alpha}$	α_0 (deg)	ω	$-m_{\dot{\alpha}}$	$-m_{\alpha}$
0·397	1·99	0·0947	1·303	0·593				
0·597	1·98	0·0655	1·249	0·586				
0·795	2·00	0·0506	1·219	0·607				
0·896	2·00	0·0460	1·472	0·651	1·00	0·0459	1·578	0·654
0·920	1·97	0·0452	1·771	0·686				
0·946	1·98	0·0443	2·116	0·721	1·00	0·0440	2·398	0·708
0·946	2·00	0·0439	2·142	0·720				
0·969	1·96	0·0434	1·969	0·717				
0·969	1·99	0·0435	2·291	0·712				
0·994	1·99	0·0423	1·477	0·794	1·00	0·0425	1·974	0·789
1·042	1·99	0·0415	0·826	1·028	1·00	0·0415	0·824	1·010
1·067					1·00	0·0409	0·615	0·973
1·092	2·00	0·0400	0·623	1·021	0·98	0·0400	0·634	0·965
1·092					1·00	0·0400	0·633	0·957
1·117	2·01	0·0393	0·623	0·989	1·00	0·0394	0·678	0·926

$h = 0\cdot7785, f = 26$ c/s (nominal)

M	α_0 (deg)	ω	$-m_{\dot{\alpha}}$	$-m_{\alpha}$	α_0 (deg)	ω	$-m_{\dot{\alpha}}$	$-m_{\alpha}$
0·397	1·96	0·0863	0·174	−0·656				
0·597	1·96	0·0582	0·329	−0·682				
0·695	1·98	0·0503	0·603	−0·711				
0·795	1·98	0·0443	0·792	−0·728				
0·896	1·96	0·0397	1·015	−0·787	0·99	0·0398	0·923	−0·789
0·896	1·99	0·0398	—	−0·779				
0·946	1·99	0·0379	1·180	−0·765	1·00	0·0379	1·139	−0·756
0·994	1·99	0·0364	1·081	−0·723	0·98	0·0368	1·013	−0·716
1·042	1·99	0·0351	0·907	−0·655	0·99	0·0351	0·882	−0·659
1·067	1·95	0·0345	0·898	−0·638				
1·092	1·99	0·0337	0·740	−0·621	0·99	0·0338	0·633	−0·633
			0·777					
1·117	1·96	0·0332	1·908	−0·622				
			2·171					
1·117	1·99	0·0331	1·076	−0·620				

TABLE 2—*continued*

Arrowhead No. 2 *L.E. Sweep* 49·4°

h = 0·3535, f = 28 c/s (nominal)

M	α_0 (deg)	ω	$-m_{\dot{\alpha}}$	$-m_{\alpha}$	α_0 (deg)	ω	$-m_{\dot{\alpha}}$	$-m_{\alpha}$
0·397	1·97	0·0945	1·181	0·590				
0·397	1·97	0·0945	1·237	0·617				
0·597	1·98	0·0649	1·143	0·618				
0·795	1·97	0·0505	1·081	0·664				
0·795	1·99	0·0507	1·192	0·657				
0·896	1·97	0·0455	1·248	0·690	1·00	0·0461	1·307	0·689
0·896	1·99	0·0461	1·270	0·699				
0·920	1·97	0·0447	—	0·716				
0·946	1·97	0·0440	1·499	0·742	0·99	0·0444	1·597	0·742
0·946	1·97	0·0437	1·461	0·748				
0·969	1·94	0·0435	1·460	0·770				
0·969	1·98	0·0431	1·406	0·780				
0·994	1·97	0·0423	1·536	0·844	0·99	0·0431	1·627	0·826
1·018	1·97	0·0417	1·552	0·881				
1·042	1·94	0·0414	1·525	0·936	0·99	0·0414	1·355	0·925
1·042	1·98	0·0413	1·638	0·934				
1·067	1·98	0·0405	1·240	1·018				
1·092	1·97	0·0402	0·810	1·147	0·99	0·0405	0·809	1·160
1·117	1·92	0·0397	{ 0·702	1·171				
			0·796					
1·117	1·99	0·0399	0·682	1·179				

h = 0·9785, f = 26 c/s (nominal)

M	α_0 (deg)	ω	$-m_{\dot{\alpha}}$	$-m_{\alpha}$	α_0 (deg)	ω	$-m_{\dot{\alpha}}$	$-m_{\alpha}$
0·397	2·05	0·0854	0·216	−0·569				
0·597	1·94	0·0575	0·364	−0·584				
0·695	1·96	0·0497	0·507	−0·597				
0·795	1·94	0·0440	0·737	−0·615				
0·844	1·98	0·0414	0·771	−0·628				
0·896	1·96	0·0395	0·786	−0·633	0·98	0·0398	1·082	0·631
0·896	1·98	0·0397	1·038	−0·636				
0·920	1·95	0·0386	0·839	−0·639				
0·946	1·98	0·0374	0·943	−0·647	0·99	0·0378	0·954	0·644
0·969	1·99	0·0371	1·145	−0·631				
0·994	1·97	0·0363	0·889	−0·603	0·99	0·0362	0·944	0·594
0·994	1·97	0·0360	0·867	−0·597				
1·018	1·99	0·0356	0·895	−0·559				
1·042	1·97	0·0350	0·910	−0·526	0·97	0·0350	1·188	0·507
1·042	1·97	0·0347	0·643	−0·524				
1·067	1·97	0·0341	1·692	−0·485	0·99	0·0345	1·536	0·487
1·092	1·96	0·0336	{ 0·727	−0·454	0·98	0·0338	3·897	0·458
			0·942					
			1·240					
1·092	1·97	0·0334	1·671	−0·461				
1·092	1·98	0·0338	2·434	−0·458				
1·117	1·96	0·0329	{ 0·708	−0·451				
			1·787					
			1·796					
1·117	1·97	0·0331	4·162	−0·456				

TABLE 2—*continued*

Arrowhead No. 3 *L.E. Sweep* 59·03°

h = 0·5493, f = 28 c/s (nominal)

M	α_0 (deg)	ω	$-m_{\dot{\alpha}}$	$-m_{\alpha}$	α_0 (deg)	ω	$-m_{\dot{\alpha}}$	$-m_{\alpha}$
0·397	1·94	0·0941	1·151	0·651				
0·597	1·95	0·0647	1·030	0·630				
0·795	1·93	0·0504	0·940	0·646				
0·795	1·97	0·0504	0·980	0·663				
0·844	1·97	0·0479	1·016	0·674				
0·896	1·97	0·0456	1·040	0·680	0·98	0·0457	1·063	0·686
0·946	1·94	0·0437	1·053	0·711	0·99	0·0438	1·066	0·706
0·946	1·96	0·0438	1·039	0·704				
0·994	1·92	0·0421	1·102	0·730	0·98	0·0429	1·044	0·723
1·042	1·96	0·0406	1·055	0·766	0·97	0·0404	1·105	0·766
1·042	1·97	0·0406	1·144	0·769	0·99	0·0404	1·082	—
1·092	1·94	0·0393	1·191	0·841	0·99	0·0394	1·153	0·824
1·117	1·95	0·0387	1·289	0·911				
1·117	1·97	0·0387	1·243	0·901				

h = 1·1809, f = 26 c/s (nominal)

M	α_0 (deg)	ω	$-m_{\dot{\alpha}}$	$-m_{\alpha}$	α_0 (deg)	ω	$-m_{\dot{\alpha}}$	$-m_{\alpha}$
0·397	1·97	0·0852	0·271	−0·456				
0·597	1·92	0·0576	0·321	−0·464				
0·795	1·98	0·0441	0·527	−0·470				
0·844	1·95	0·0417	0·569	—				
0·844	1·98	0·0419	0·530	−0·479				
0·896	1·94	0·0398	0·556	−0·480	0·98	0·0399	0·503	−0·475
0·896	1·96	0·0405	0·519	−0·476				
0·946	1·97	0·0380	0·572	−0·478	0·98	0·0379	0·526	−0·475
0·994	1·95	0·0364	0·587	−0·482	0·96	0·0363	0·637	−0·478
0·994	1·98	0·0363	0·590	−0·480	0·98	0·0363	0·628	−0·479
1·042	1·96	0·0350	0·506	−0·470	0·98	0·0350	0·429	−0·469
1·092	1·95	0·0336	0·487	−0·429	0·98	0·0339	0·416	−0·427
							0·487	
1·092	1·97	0·0337	0·458	−0·430				
1·117	1·96	0·0331	0·489	−0·412				

TABLE 3

Arrowhead No. 2 L.E. Sweep 49·4°—*Turbulent Boundary Layer*

$h = 0{\cdot}9785, f = 26$ c/s (nominal)

M	α_0 (deg)	ω	$-m_{\dot{\alpha}}$	$-m_{\alpha}$
0·397	1·95	0·0861	0·191	−0·562
0·795	1·95	0·0444	0·736	−0·615
0·896	1·95	0·0399	0·711	−0·627
0·994	1·95	0·0365	0·884	−0·603
1·042	1·95	0·0355	0·709	−0·545
1·092	1·96	0·0343	1·564	−0·494

TABLE 4

Aspect Ratio 3·0 Delta—Tunnel Wall Conditions

$h = 0{\cdot}2435, f = 51$ c/s (nominal)

Condition (i)—Normal slotted walls—*see* Table 2.

Condition (ii)—8 slots closed.

M	α_0 (deg)	ω	$-m_{\dot{\alpha}}$	$-m_{\alpha}$
0·397	2·05	0·1400	1·566	0·865
0·597	2·04	0·0952	1·655	0·849
0·695	2·05	0·0827	1·671	0·877
0·795	2·06	0·0733	1·724	0·919
0·896	2·06	0·0660	2·025	0·956
0·920	2·04	0·0654	2·172	0·991
0·946	2·06	0·0632	2·059	1·116
0·969	2·05	0·0627	1·516	1·242
0·994	2·02	0·0614	1·296	1·280
1·042	2·04	0·0590	1·085	1·259
1·092	2·04	0·0568	0·844	1·206

Condition (iii)—All 16 slots closed.

M	α_0 (deg)	ω	$-m_{\dot{\alpha}}$	$-m_{\alpha}$	α_0 (deg)	ω	$-m_{\dot{\alpha}}$	$-m_{\alpha}$
0·397	2·11	0·1403	1·311	0·967	1·06	0·1409	1·354	1·008
0·397	2·08	0·1406	1·379	0·927	1·04	0·1402	1·370	0·953
0·597	2·07	0·0956	1·487	0·947	1·04	0·0957	1·512	0·948
0·597	2·10	0·0953	1·510	0·927				
0·695	2·12	0·0828	1·589	0·967	1·05	0·0830	1·628	0·965
0·695	2·11	0·0827	1·517	0·957				
0·695	2·07	0·0835	1·539	0·966				
0·795	2·09	0·0739	1·653	1·024	1·05	0·0735	1·657	1·000
0·795	2·12	0·0734	1·592	1·015	1·05	0·0739	1·722	1·005
0·896	2·08	0·0668	1·924	1·085	1·05	0·0665	1·972	1·049
0·896	2·13	0·0665	1·927	1·112	1·06	0·0663	2·025	1·081

Condition (iv)—Wide slots.

M	α_0 (deg)	ω	$-m_{\dot{\alpha}}$	$-m_{\alpha}$
0·400	2·05	0·1385	1·576	0·868
0·600	2·07	0·0945	1·642	0·822
0·700	2·02	0·0822	1·703	0·855
0·800	2·07	0·0729	1·768	0·903
0·905	2·04	0·0658	2·052	0·927
0·931	2·05	0·0639	2·204	0·976
0·957	2·06	0·0625	2·045	1·104
0·984	2·07	0·0612	1·408	1·199
1·010	2·08	0·0599	1·244	1·205
1·062	2·07	0·0573	0·909	1·202
1·115	2·07	0·0550	0·641	1·178
1·115	2·02	0·0554	0·639	1·170

TABLE 4—*continued*

Aspect Ratio 3·0 *Delta—Tunnel Wall Conditions*

$h = 0{\cdot}2435, f = 27$ c/s (nominal)

Condition (i) normal slotted walls—*see* Table 2.

Condition (iii)—All 16 *slots closed.*

M	α_0 (deg)	ω	$-m_{\dot{\alpha}}$	$-m_{\alpha}$
0·397	2·12	0·0747	1·306	0·923
0·597	2·09	0·0509	1·431	0·933
0·695	2·09	0·0445	1·506	0·964
0·795	2·09	0·0397	1·624	1·013
0·896	2·11	0·0358	1·951	1·098

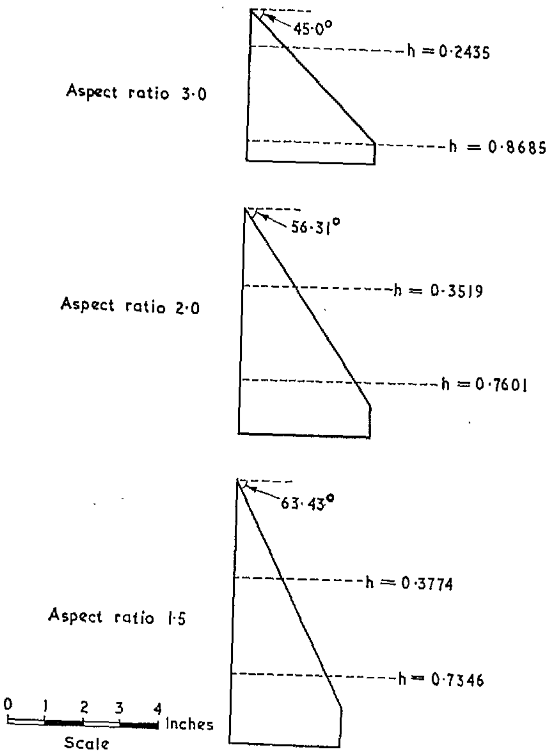

FIG. 1. Cropped-delta family: Section RAE 102, $t/c = 0 \cdot 06$.

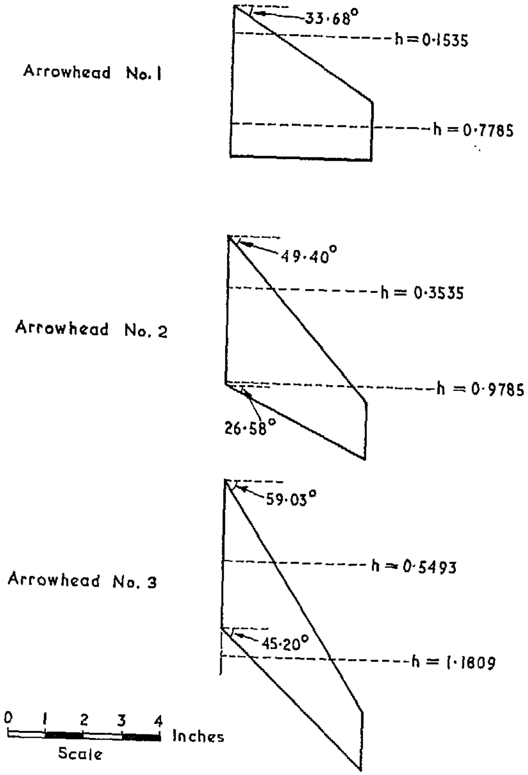

FIG. 2. Arrowhead family: Section RAE 102, $t/c = 0 \cdot 06$, Aspect ratio $2 \cdot 575$.

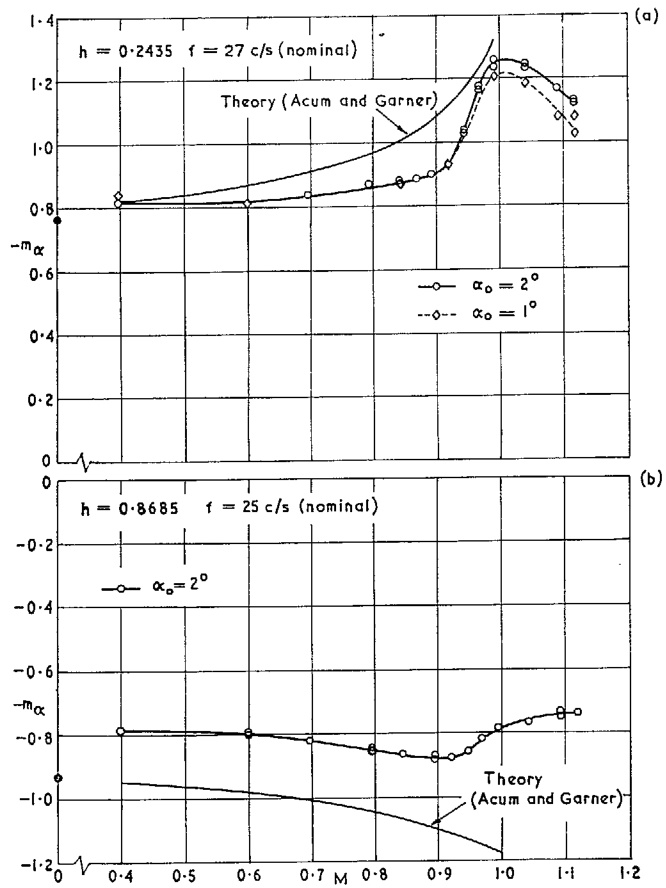

FIGS. 3a and b. Aspect ratio 3·0 delta—variation of $-m_\alpha$ with Mach number.

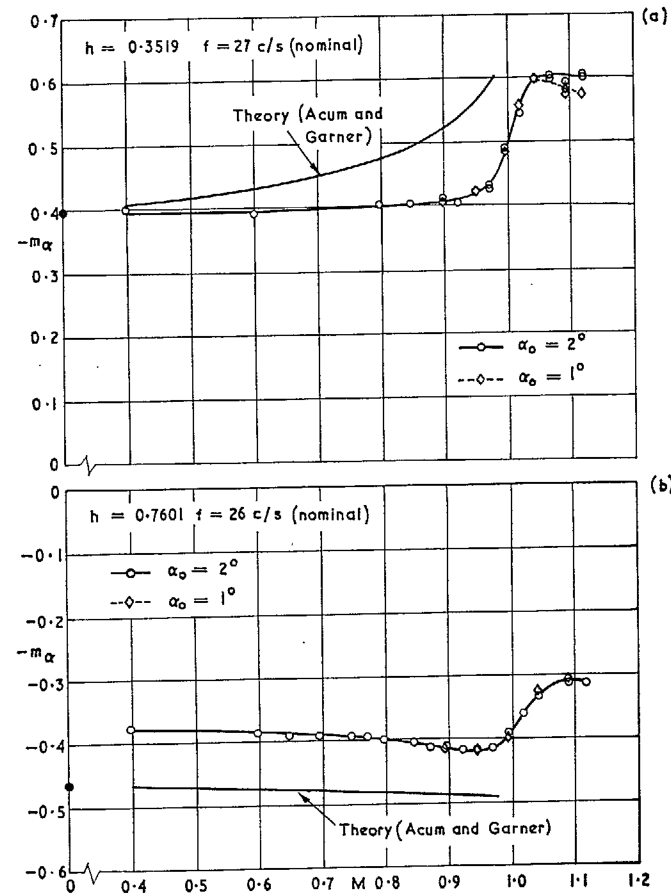

FIGS. 4a and b. Aspect ratio 2·0 delta—variation of $-m_\alpha$ with Mach number.

(90850)

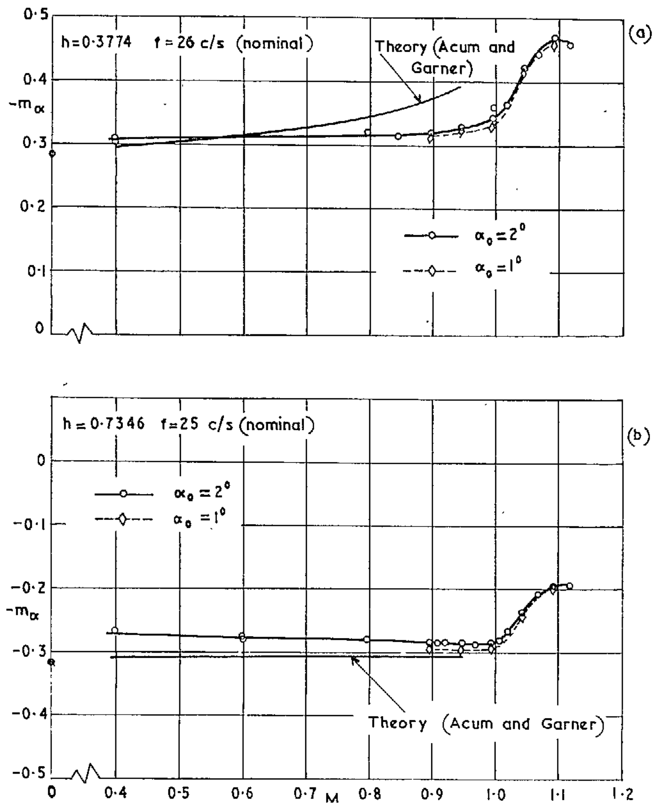

FIGS. 5a and b. Aspect ratio 1·5 delta—variation of $-m_{\alpha}$ with Mach number.

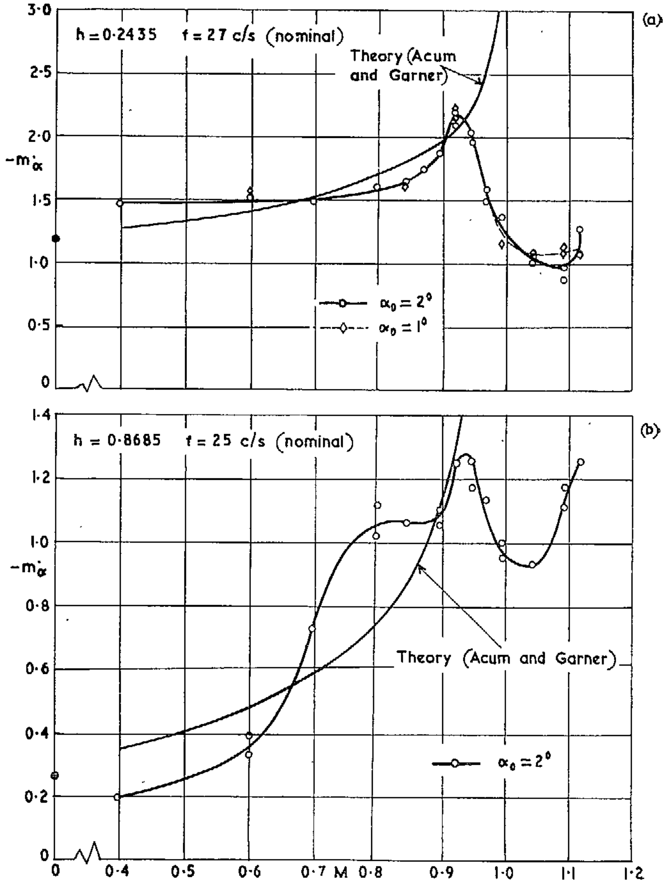

FIGS. 6a and b. Aspect ratio 3·0 delta—variation of $-m_{\dot{\alpha}}$ with Mach number.

D

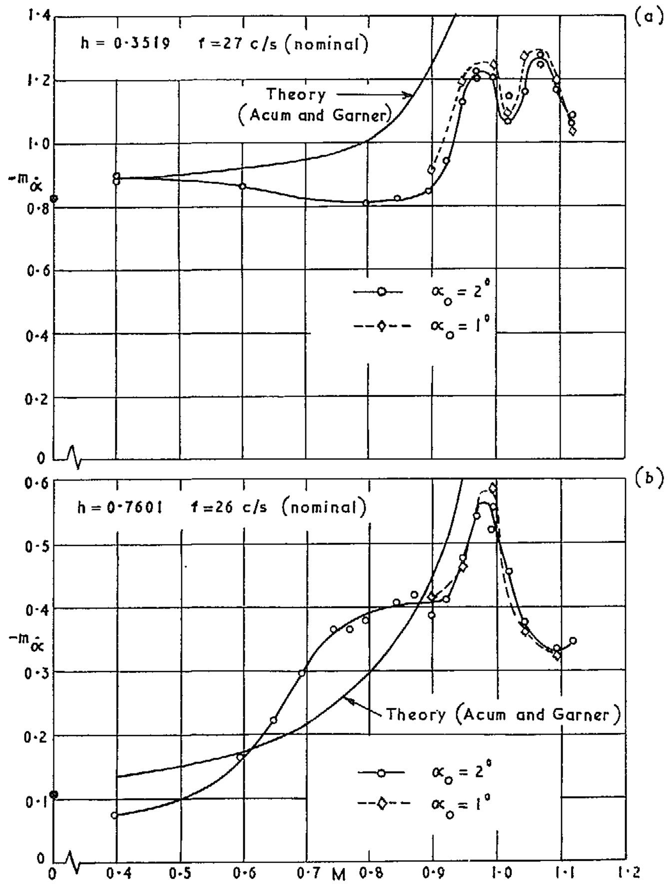

FIGS. 7a and b. Aspect ratio 2·0 delta—variation of $-m_{\dot{\alpha}}$ with Mach number.

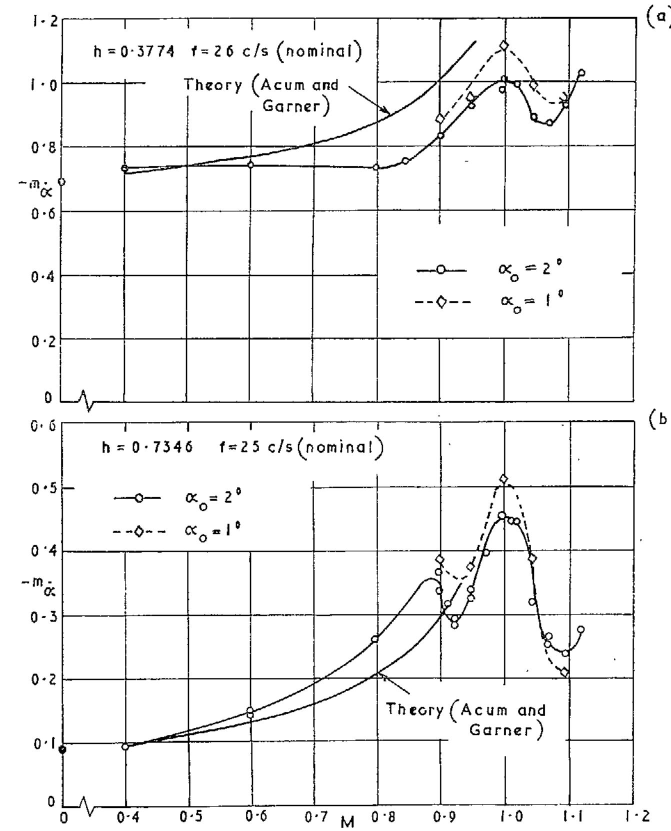

FIGS. 8a and b. Aspect ratio 1·5 delta—variation of $-m_{\dot{\alpha}}$ with Mach number.

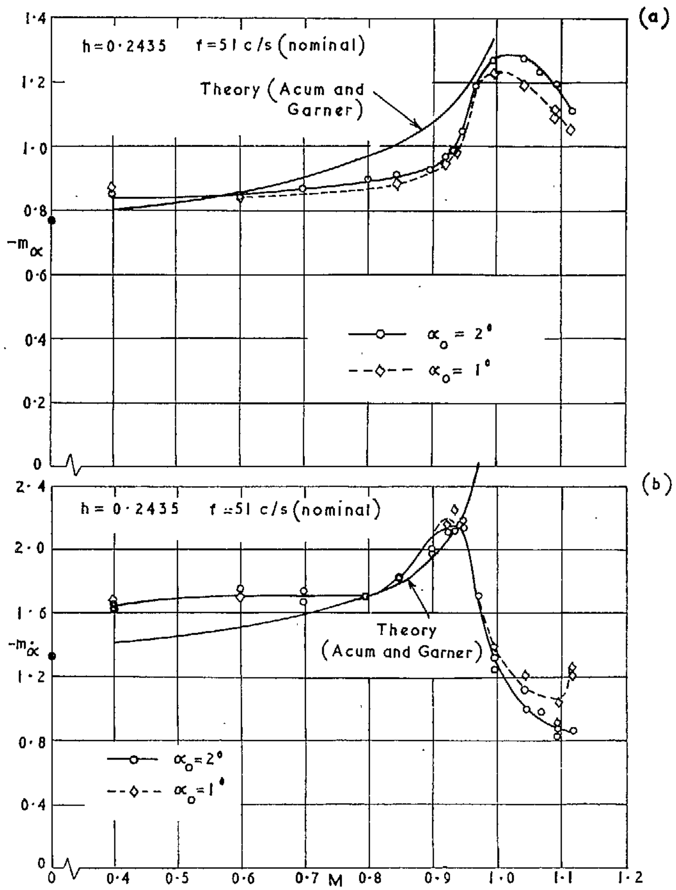

FIGS. 9a and b. Aspect ratio 3·0 delta—variation of $-m_\alpha$, $-m_{\dot\alpha}$ with Mach number.

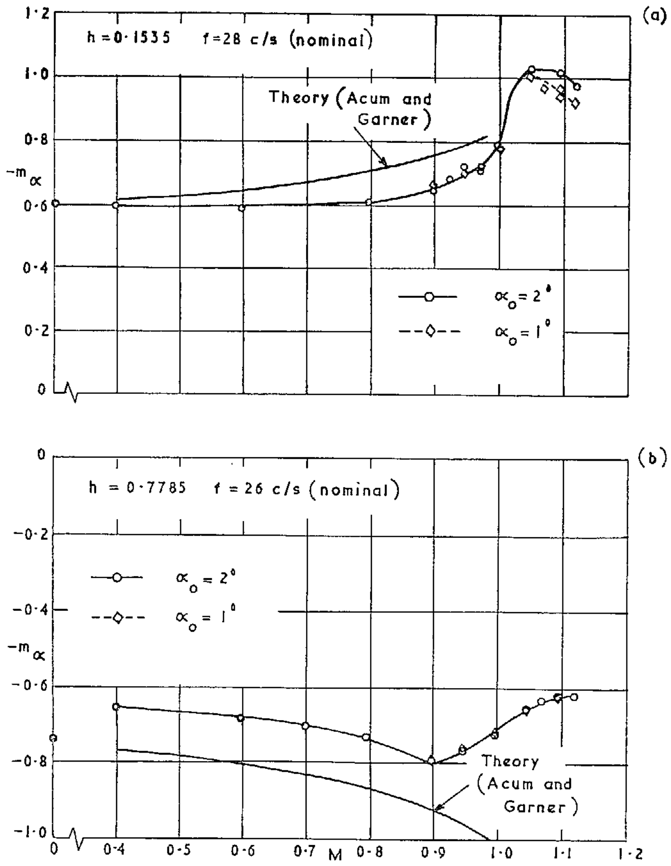

FIGS. 10a and b. Arrowhead No. 1 L.E. sweep 33·68° —variation of $-m_\alpha$ with Mach number.

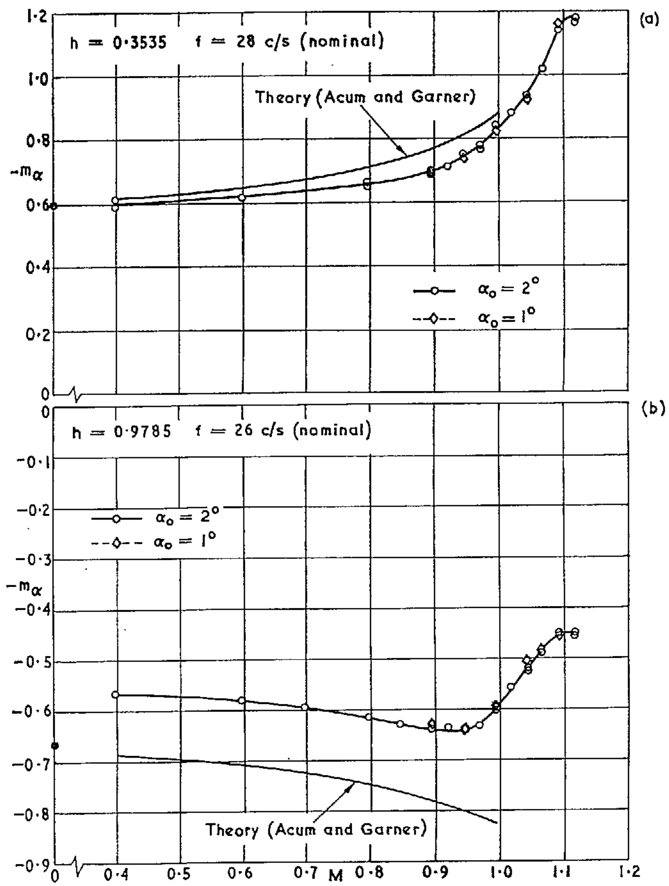

FIGS. 11a and b. Arrowhead No. 2 L.E. sweep 49·40° —variation of $-m_\alpha$ with Mach number.

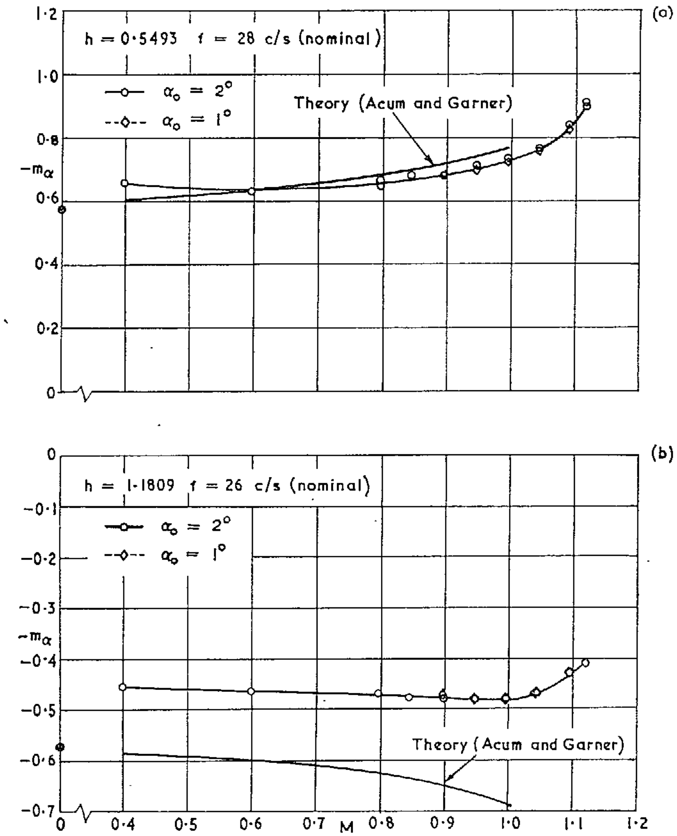

FIGS. 12a and b. Arrowhead No. 3 L.E. sweep 59·03° —variation of $-m_\alpha$ with Mach number.

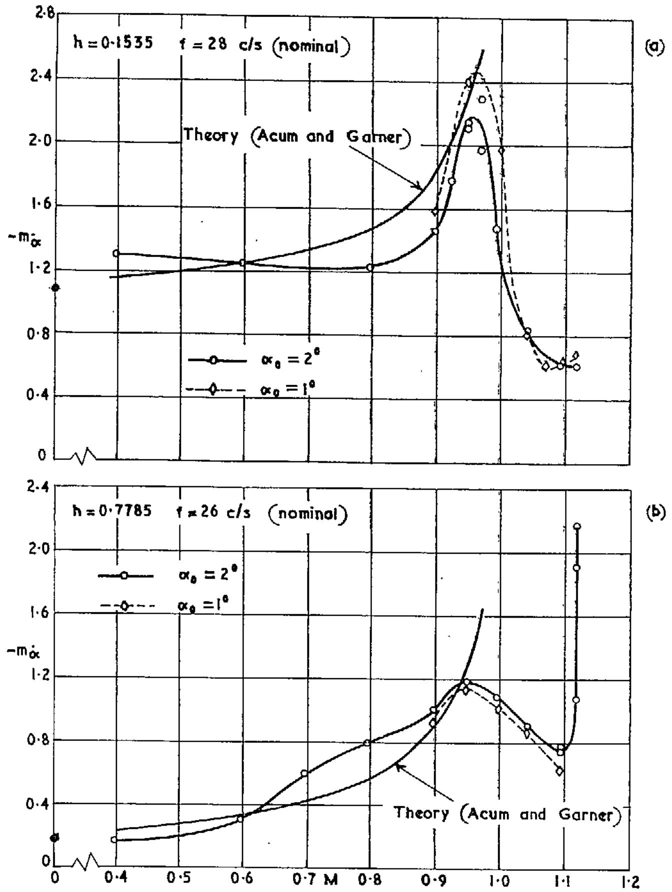

FIGS. 13a and b. Arrowhead No. 1 L.E. sweep 33·68° —variation of $-m_{\dot{\alpha}}$ with Mach number.

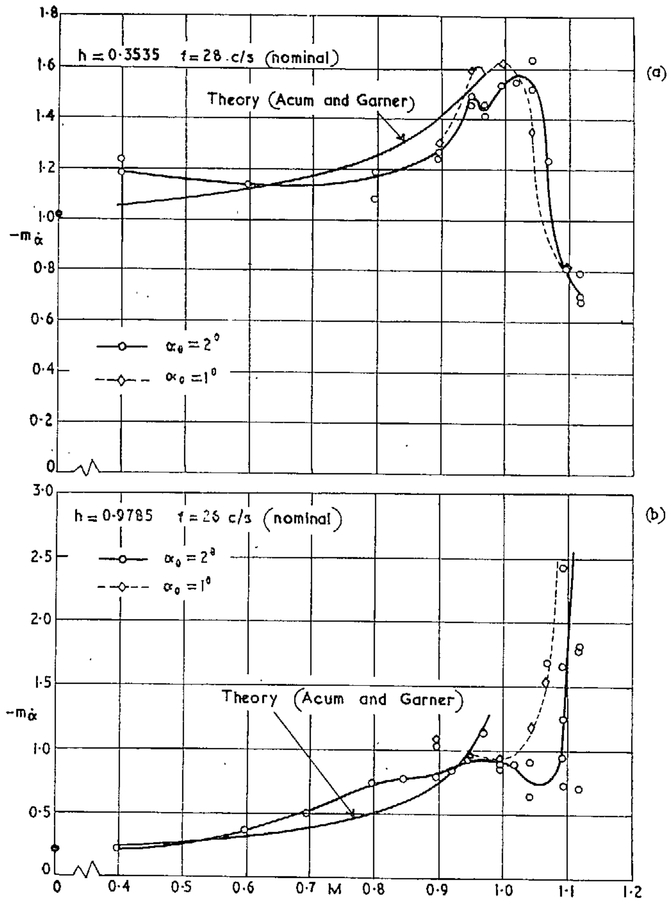

FIGS. 14a and b. Arrowhead No. 2 L.E. sweep 49·40° —variation of $-m_{\dot{\alpha}}$ with Mach number.

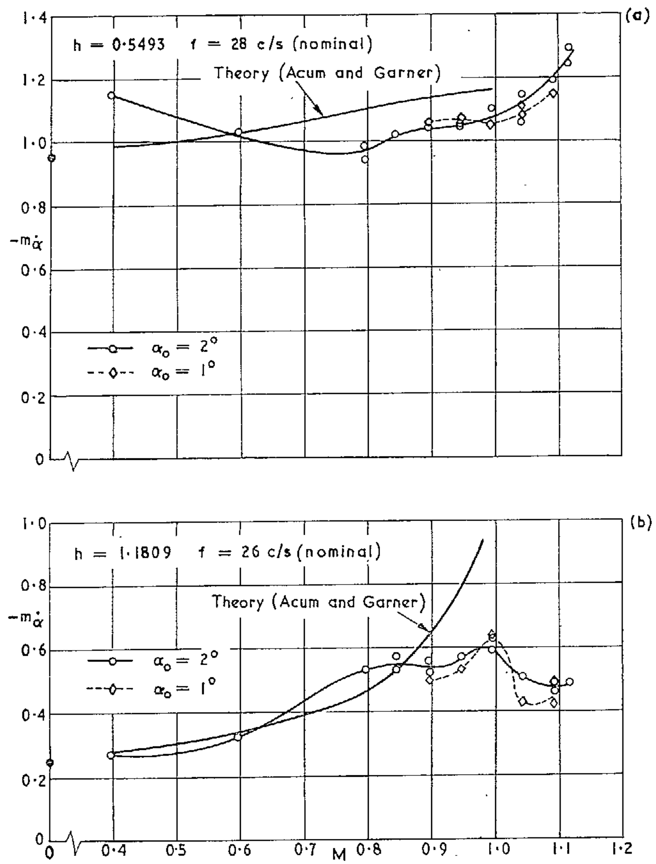

FIGS. 15a and b. Arrowhead No. 3 L.E. sweep 59·03° —variation of $-m_{\dot\alpha}$ with Mach number.

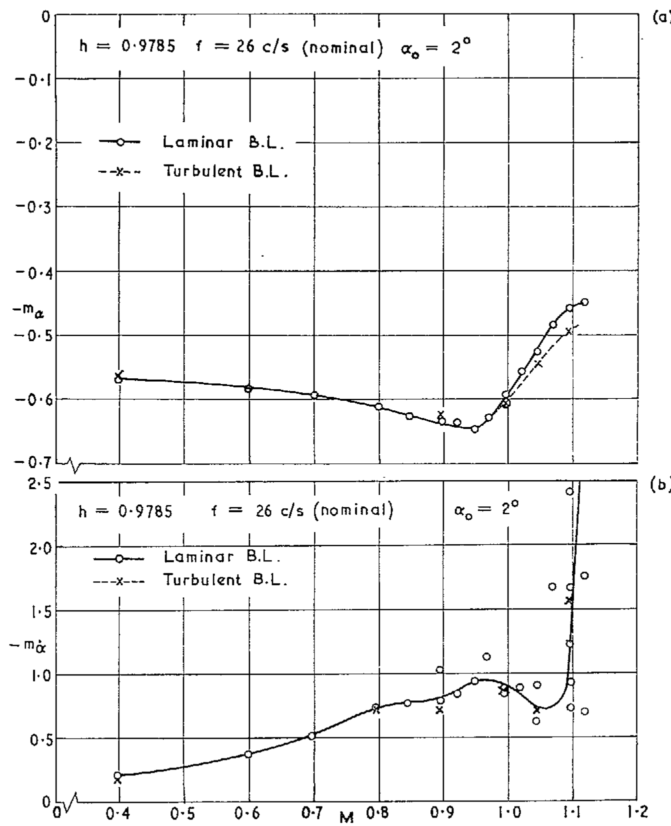

FIGS. 16a and b. Arrowhead No. 2 L.E. sweep 49·4° —effect of turbulent boundary layer on $-m_\alpha$, $-m_{\dot\alpha}$.

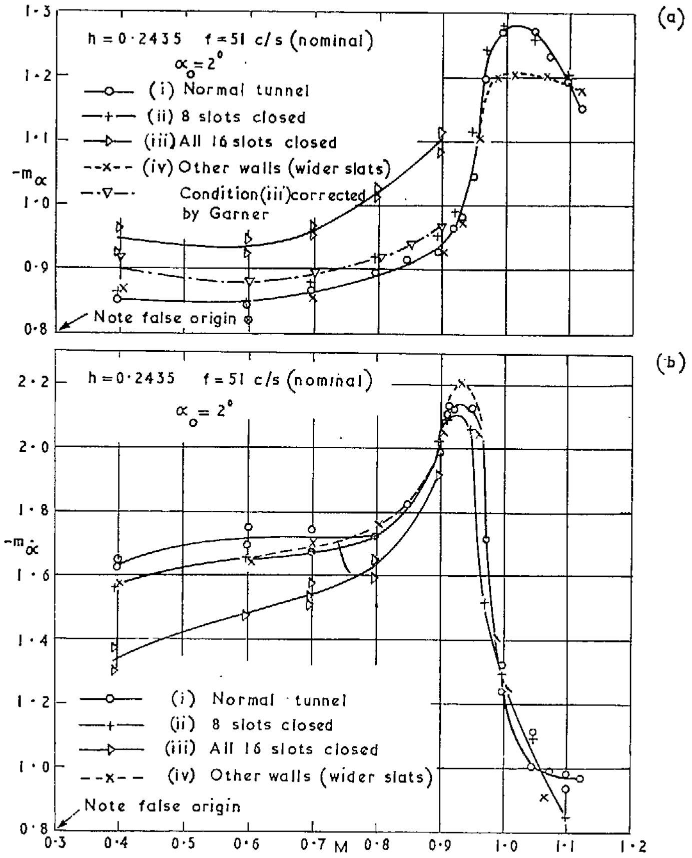

FIGS. 17a and b. Aspect ratio 3·0 delta—effect of tunnel wall condition on $-m_\alpha$, $-m_{\dot\alpha}$.

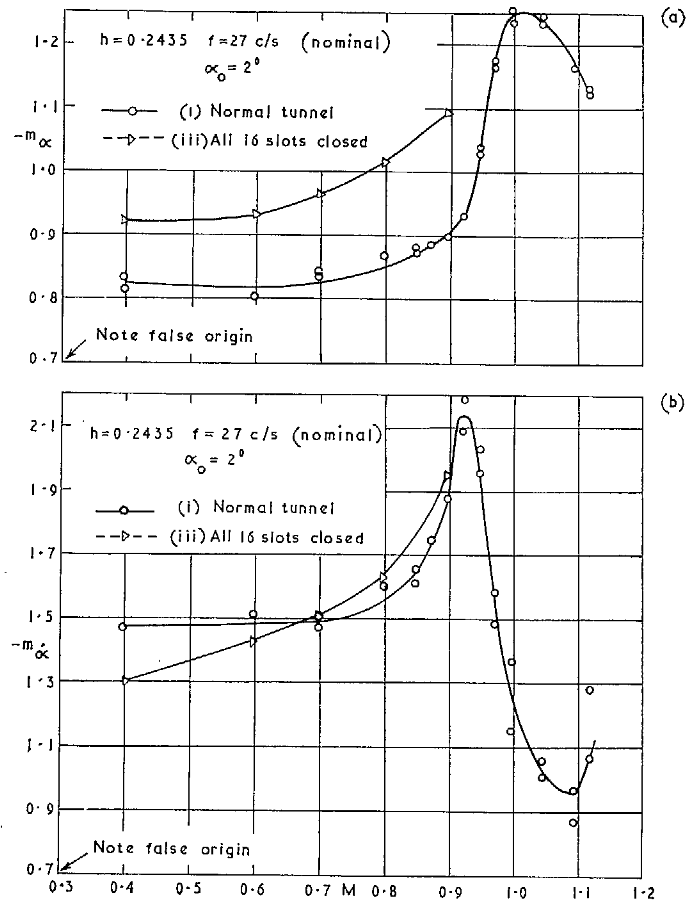

FIGS. 18a and b. Aspect ratio 3·0 delta—effect of tunnel wall condition on $-m_\alpha$, $-m_{\dot\alpha}$.

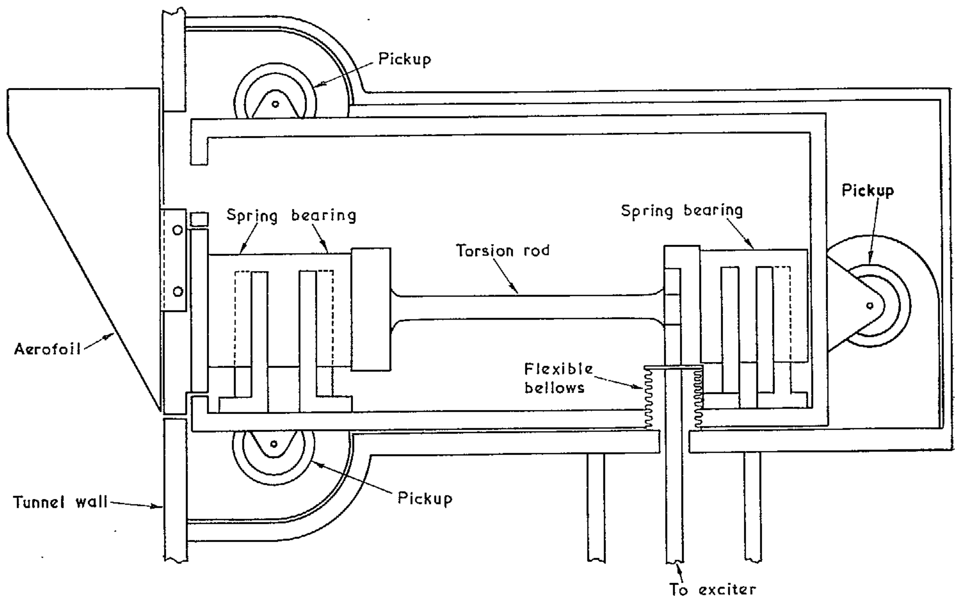

FIG. 19. General arrangement of apparatus—Side view.

(90850) Wt. 66/2301 K5 2/65 Hw.

Publications of the Aeronautical Research Council

ANNUAL TECHNICAL REPORTS OF THE AERONAUTICAL RESEARCH COUNCIL (BOUND VOLUMES)

1942 Vol. I. Aero and Hydrodynamics, Aerofoils, Airscrews, Engines. 75*s.* (post 2*s.* 9*d.*)
Vol. II. Noise, Parachutes, Stability and Control, Structures, Vibration, Wind Tunnels. 47*s.* 6*d.* (post 2*s.* 3*d.*)

1943 Vol. I. Aerodynamics, Aerofoils, Airscrews. 80*s.* (post 2*s.* 6*d.*)
Vol. II. Engines, Flutter, Materials, Parachutes, Performance, Stability and Control, Structures. 90*s.* (post 2*s.* 9*d.*)

1944 Vol. I. Aero and Hydrodynamics, Aerofoils, Aircraft, Airscrews, Controls. 84*s.* (post 3*s.*)
Vol. II. Flutter and Vibration, Materials, Miscellaneous, Navigation, Parachutes, Performance, Plates and Panels, Stability, Structures, Test Equipment, Wind Tunnels. 84*s.* (post 3*s.*)

1945 Vol. I. Aero and Hydrodynamics, Aerofoils. 130*s.* (post 3*s.* 6*d.*)
Vol. II. Aircraft, Airscrews, Controls. 130*s.* (post 3*s.* 6*d.*)
Vol. III. Flutter and Vibration, Instruments, Miscellaneous, Parachutes, Plates and Panels, Propulsion. 130*s.* (post 3*s.* 3*d.*)
Vol. IV. Stability, Structures, Wind Tunnels, Wind Tunnel Technique. 130*s.* (post 3*s.* 3*d.*)

1946 Vol. I. Accidents, Aerodynamics, Aerofoils and Hydrofoils. 168*s.* (post 3*s.* 9*d.*)
Vol. II. Airscrews, Cabin Cooling, Chemical Hazards, Controls, Flames, Flutter, Helicopters, Instruments and Instrumentation, Interference, Jets, Miscellaneous, Parachutes. 168*s.* (post 3*s.* 3*d.*)
Vol. III. Performance, Propulsion, Seaplanes, Stability, Structures, Wind Tunnels. 168*s.* (post 3*s.* 6*d.*)

1947 Vol. I. Aerodynamics, Aerofoils, Aircraft. 168*s.* (post 3*s.* 9*d.*)
Vol. II. Airscrews and Rotors, Controls, Flutter, Materials, Miscellaneous, Parachutes, Propulsion, Seaplanes, Stability, Structures, Take-off and Landing. 168*s.* (post 3*s.* 9*d.*)

1948 Vol. I. Aerodynamics, Aerofoils, Aircraft, Airscrews, Controls, Flutter and Vibration, Helicopters, Instruments, Propulsion, Seaplane, Stability, Structures, Wind Tunnels. 130*s.* (post 3*s.* 3*d.*)
Vol. II. Aerodynamics, Aerofoils, Aircraft, Airscrews, Controls, Flutter and Vibration, Helicopters, Instruments, Propulsion, Seaplane, Stability, Structures, Wind Tunnels. 110*s.* (post 3*s.* 3*d.*)

Special Volumes

Vol. I. Aero and Hydrodynamics, Aerofoils, Controls, Flutter, Kites, Parachutes, Performance, Propulsion, Stability. 126*s.* (post 3*s.*)
Vol. II. Aero and Hydrodynamics, Aerofoils, Airscrews, Controls, Flutter, Materials, Miscellaneous, Parachutes, Propulsion, Stability, Structures. 147*s.* (post 3*s.*)
Vol. III. Aero and Hydrodynamics, Aerofoils, Airscrews, Controls, Flutter, Kites, Miscellaneous, Parachutes, Propulsion, Seaplanes, Stability, Structures, Test Equipment. 189*s.* (post 3*s.* 9*d.*)

Reviews of the Aeronautical Research Council

1939–48 3*s.* (post 6*d.*) 1949–54 5*s.* (post 5*d.*)

Index to all Reports and Memoranda published in the Annual Technical Reports

1909–1947 R. & M. 2600 (out of print)

Indexes to the Reports and Memoranda of the Aeronautical Research Council

Between Nos. 2351–2449	R. & M. No. 2450	2*s.* (post 3*d.*)
Between Nos. 2451–2549	R. & M. No. 2550	2*s.* 6*d.* (post 3*d.*)
Between Nos. 2551–2649	R. & M. No. 2650	2*s.* 6*d.* (post 3*d.*)
Between Nos. 2651–2749	R. & M. No. 2750	2*s.* 6*d.* (post 3*d.*)
Between Nos. 2751–2849	R. & M. No. 2850	2*s.* 6*d.* (post 3*d.*)
Between Nos. 2851–2949	R. & M. No. 2950	3*s.* (post 3*d.*)
Between Nos. 2951–3049	R. & M. No. 3050	3*s.* 6*d.* (post 3*d.*)
Between Nos. 3051–3149	R. & M. No. 3150	3*s.* 6*d.* (post 3*d.*)

HER MAJESTY'S STATIONERY OFFICE

from the addresses overleaf

Printed and published by
HER MAJESTY'S STATIONERY OFFICE

To be purchased from
York House, Kingsway, London w.c.2
423 Oxford Street, London w.1
13A Castle Street, Edinburgh 2
109 St. Mary Street, Cardiff
39 King Street, Manchester 2
50 Fairfax Street, Bristol 1
35 Smallbrook, Ringway, Birmingham 5
80 Chichester Street, Belfast 1
or through any bookseller

Printed in England

R. & M. No. 3397

S.O. Code No. 23-3392